

# Distributionally Consistent Simulation of Naturalistic Driving Environment for Autonomous Vehicle Testing

Xintao Yan, Shuo Feng, *Member, IEEE*, Haowei Sun, Henry X. Liu, *Member, IEEE*

**Abstract**—Microscopic traffic simulation provides a controllable, repeatable, and efficient testing environment for autonomous vehicles (AVs). To evaluate AVs' safety performance unbiasedly, the probability distributions of environment statistics in the simulated naturalistic driving environment (NDE) need to be consistent with those from the real-world driving environment. However, although human driving behaviors have been extensively investigated in the transportation engineering field, most existing models were developed for traffic flow analysis without considering the distributional consistency of driving behaviors, which could cause significant evaluation biasedness for AV testing. To fill this research gap, a distributionally consistent NDE modeling framework is proposed in this paper. Using large-scale naturalistic driving data, empirical distributions are obtained to construct the stochastic human driving behavior models under different conditions. To address the error accumulation problem during the simulation, an optimization-based method is further designed to refine the empirical behavior models. Specifically, the vehicle state evolution is modeled as a Markov chain and its stationary distribution is twisted to match the distribution from the real-world driving environment. The framework is evaluated in the case study of a multi-lane highway driving simulation, where the distributional accuracy of the generated NDE is validated and the safety performance of an AV model is effectively evaluated.

**Index Terms**—Autonomous vehicle, driving behavior, naturalistic driving environment, simulation, testing and evaluation

## I. INTRODUCTION

TESTING and evaluation is a critical step in the development and deployment of autonomous vehicles (AVs), which has received extensive attention from both the industry and academia in recent years [1]–[14]. Prevailing methods test AVs in the naturalistic driving environment (NDE), observe their performance, and make statistical comparisons to human driving performance [13]. Due to the rareness of safety-critical events, however, it has been pointed out that hundreds of millions and sometimes hundreds of billions of miles would

be required in NDE to demonstrate the safety performance of AVs at the level of human-driven vehicles, which is intolerably inefficient for the real-world testing [1]. Therefore, testing AVs in NDE simulations has attracted increasing attention because of the advantages of controllability, repeatability, and efficiency [13], [15].

The key to simulation testing is the trustworthiness of the testing results. As pointed out in various domains [15]–[18], the simulation-to-reality gap could hinder and even mislead the training and testing process of an agent. To fill this gap, existing studies have paid much attention to the fidelity of vehicle dynamics, sensor models, and photorealistic images based on techniques such as computer graphics, physics-based modeling, and data augmentation [15], [19], [20]. However, how to model the naturalistic behavior of human-driven vehicles with high fidelity still remains an open question. To answer this question, many AV companies tried to replay human driving behaviors according to the logged data collected from the real-world driving environment. However, as the human driving behaviors are pre-determined in the logged data, they cannot interact with AV models, which severely limits the scenarios that can be simulated. To address this issue, the human driving models developed in the transportation engineering field have been applied, such as the Intelligent Driving Model (IDM) [21] and MOBIL [22] models. However, although these models can interact with AV models, they were designed for traffic flow analysis purposes such as reproducing traffic oscillations and the fundamental diagram, which are not suitable for the AV simulation testing (see Section II for more details of related studies).

The AV simulation testing brings brand new requirements for the NDE modeling. To evaluate AVs' safety performance quantitatively, the accident rate of AVs in NDE is usually utilized [2], [7], [8], [13]. As the human driving behaviors significantly affect the response and performance of AVs, estimating the accident rate accurately requires the NDE model in simulation to be distributionally consistent with the real-world driving environment. Specifically, let  $X$  denote the variables that define the environment, such as the behaviors of human drivers. Then, testing an AV in NDE is essential to sample  $X$  from its underlying distribution, denoted as  $X \sim P(X)$ , to estimate its performance  $\mu_E^\kappa$  by

$$\mu_E^\kappa := \mathbb{E}_X(\phi_E^\kappa(X)) \approx \frac{1}{n} \sum_{i=1}^n \phi_E^\kappa(X_i) \approx \frac{m}{n}, X_i \sim P(X), \quad (1)$$

This research was partially funded by the US Department of Transportation (USDOT) Region 5 University Transportation Center: Center for Connected and Automated Transportation (CCAT) of the University of Michigan. (Corresponding author: Shuo Feng.)

Xintao Yan and Haowei Sun are with the Department of Civil and Environmental Engineering, University of Michigan, Ann Arbor, MI 48109 USA, (e-mail: xintaoy@umich.edu; haowei@umich.edu).

Shuo Feng is with the University of Michigan Transportation Research Institute, Ann Arbor, MI 48109 USA, (e-mail: fshuo@umich.edu).

Henry X. Liu is with the Department of Civil and Environmental Engineering, MCity, and also University of Michigan Transportation Research Institute, University of Michigan, Ann Arbor, MI 48109 USA, (e-mail: henryliu@umich.edu).

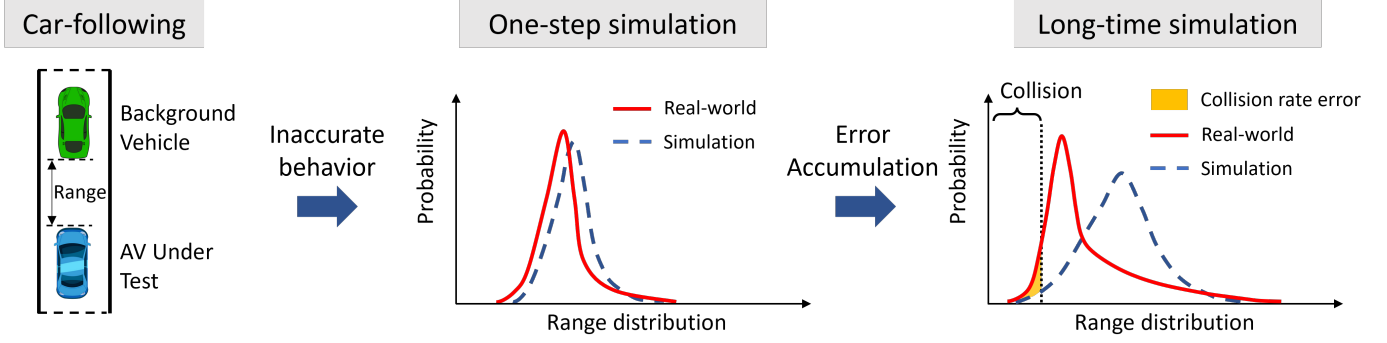


Fig. 1. Illustration of the distribution inconsistency that might mislead AV development and deployment.

where  $E$  denotes the event of interest (e.g., crash),  $\kappa$  denotes the AV agent under test,  $\phi_E^\kappa(X)$  denotes the AV performance at the environment specified by  $X$ ,  $n$  denotes the number of tests, and  $m$  denotes the number of event  $E$  occurred during tests. According to the Monte Carlo method [23], only with the accurate distribution  $P(X)$  in the simulation, the estimation of  $\mu_E^\kappa$  can be statistically accurate. Therefore, the AV simulation testing requires distributionally consistent NDE models, which are significantly different from those for traffic flow analysis.

To further illustrate the new requirements, we consider a simple car-following scenario, where the leading vehicle is a human-driven vehicle and the following vehicle is an AV, as shown in Fig. 1. In the real-world driving environment, the behaviors of the leading vehicle could have an underlying distribution, which leads to the range distribution between two vehicles after one timestep (see Fig. 1, middle, red curve). If the NDE model cannot accurately represent the stochastic behaviors of the leading vehicle, there could exist an inconsistency between the range distributions in simulation (Fig. 1, middle, blue dashed line) and real-world. After several time steps, this inconsistency will be accumulated and amplified, which could lead to significant estimation errors of the accident rate (Fig. 1, right, yellow area). In this example, the accident rate will be underestimated in simulation, which could mislead the further development and deployment of AVs. Therefore, a realistic NDE with distributionally consistent environment statistics is critical for AV testing, which is a challenging requirement. To the best of our knowledge, we are the first to identify and systematically investigate this new NDE modeling requirement, and there is no existing method that can fulfill this requirement.

To fill this research gap, we propose a data-driven optimization-based NDE modeling framework in this paper, which can ensure the distributional consistency of vehicle microscopic behaviors. The overall pipeline of the framework includes two major steps as shown in Fig. 2. In the first data-driven step, we propose to directly construct human driving behavior models using empirical distributions from the large-scale naturalistic driving data (NDD). Specifically, the driving behaviors are modeled by two longitudinal models (i.e., free driving and car following) and four lateral models considering different driving situations, and each model is described as action distributions for different states. For example, the

car-following behaviors can be modeled by the acceleration distribution of the following vehicle conditional on different self speeds, relative speeds, and relative distances with the preceding vehicle. These empirical behavior models serve as basic models. If the dataset is sufficiently accurate, diverse, and large, the empirical distributions can accurately characterize human driving behaviors in different situations. However, due to the limitation of data quantity and unavoidable data noise, the obtained empirical distributions may still have small inaccuracy compared with the ground truth. As illustrated in Fig. 1, the small inaccuracy can be accumulated and compounded with the simulation, so the resultant simulation environment will deviate from the realistic environment.

To further tackle the error accumulation issue, the second step of the framework is to refine empirical behavior models to minimize the accumulated errors using optimization methods. To achieve this goal, the key is to model the long-term effects of the error accumulation. In this study, by modeling the vehicle state evolution as a Markov chain, the long-term effects of the error accumulation could be modeled based on the stationary distribution of the Markov chain. Then, an optimization problem can be formulated to minimize the accumulated errors by adjusting the empirical behavior models. In this way, the error accumulation could be reduced, which results in the NDE model with more accurate distributions. This provides opportunities to conduct high-fidelity long-time simulation for full-length trip evaluation of AV's performance [24]. Using the large-scale real-world NDD collected by the University of Michigan, Ann Arbor, we validate the performance of the proposed method for a multilane highway driving environment. Compared with existing models, the proposed method demonstrates superior performance regarding the distributional accuracy. To further validate the capability for AV testing, the generated NDE is also utilized to test the safety performance of an AV agent.

In summary, the main contributions of this paper are threefold: first, the new requirements of NDE modeling are identified for AV testing purposes, which cannot be satisfied by most existing methods; second, a novel modeling framework is proposed to generate the NDE that is distributionally consistent with the real-world driving environment; third, the proposed method is validated using large-scale real-world NDD and the generated NDE is further validated by testing

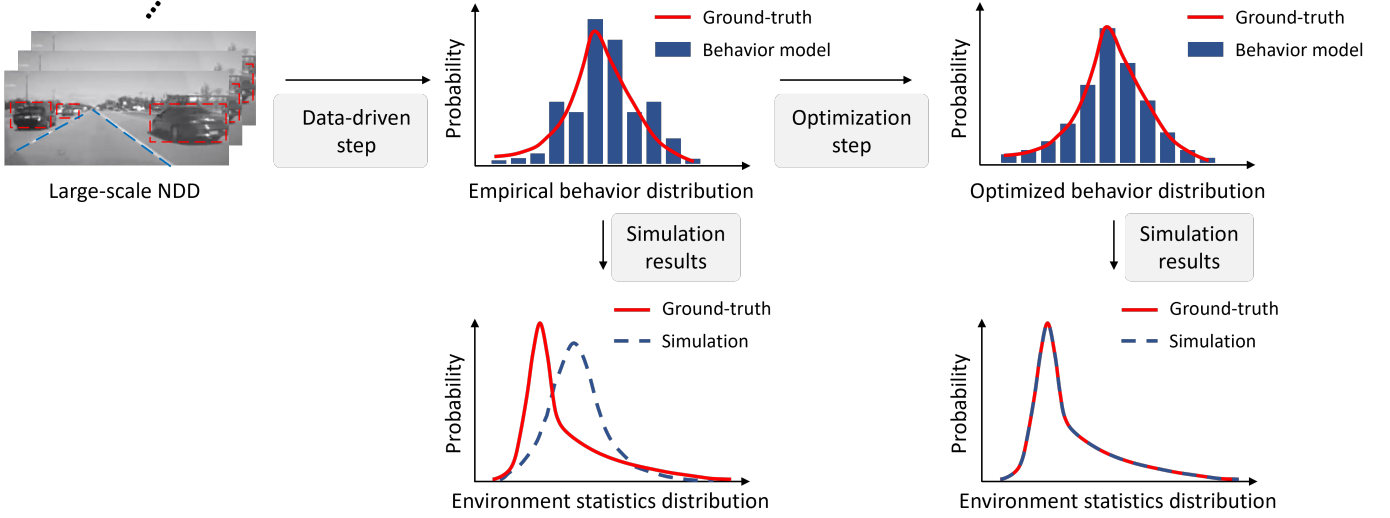


Fig. 2. Proposed framework pipeline.

an AV model.

The rest of this paper is organized as follows. In Section II, we provide a brief review of existing NDE modeling methods. In Section III, we introduce the data-driven step to construct empirical behavior models using large-scale real-world NDD and evaluate their performances in a multilane highway driving environment simulation. In Section IV, to account for the error accumulation problem, the robust modeling step is proposed to optimize the empirical behavior models to obtain a distributionally consistent NDE. In Section V, the performance of the proposed method is validated and compared with existing models. An AV testing experiment is further conducted to demonstrate the capability of the proposed NDE in this section. Finally, Section VI concludes the paper and lays out some future directions.

## II. RELATED WORK

In this section, we provide a brief overview of existing driving behavior models, especially focusing on how the behavior stochasticity is modeled and whether they can achieve distribution-level accuracy. A general form of the existing driving behavior model can be expressed by

$$u(t) = \psi(S(t), \theta(t)) + \epsilon(t), \quad (2)$$

where  $t$  denotes the time,  $u(t)$  denotes the action (e.g., longitudinal acceleration) of the vehicle at the  $t$ -th time instance,  $S(t)$  denotes the states of the ego-vehicle and surrounding vehicles that have the influence on the ego-vehicle's decision making,  $\psi(\cdot)$  denotes the model that maps from the state space to the action space,  $\theta(t)$  denotes model parameters that could be deterministic or stochastic, and  $\epsilon(t)$  denotes the additive noise term.

Most traditional models [21], [22], [25]–[27] are deterministic and cannot capture the stochastic nature of human driving behaviors. For these models, the model parameters  $\theta$  remain fixed during the simulation and no external noise

term  $\epsilon$  is added. Although the parameters of these models can be calibrated using real-world data [28]–[32], they cannot capture the stochastic behaviors of human drivers. Recently, increasing studies have used machine learning-based methods to fit the behavior model  $\psi$  using neural networks [33]–[37]. By utilizing large-scale naturalistic driving datasets, these methods aim to better reproduce the observed trajectories of human drivers. However, the problem of lacking accurate stochasticity still remains unsolved.

The stochasticity can be incorporated into the model to a certain extent by introducing external noise term  $\epsilon(t)$  and/or stochasticity to model parameters  $\theta(t)$ . For external noise  $\epsilon(t)$ , the most commonly used one is the Gaussian noise [38]–[42]. However, the external addition of the Gaussian noise cannot realistically depict human driving behaviors since the interaction in different driving conditions is highly complex and does not always follow the simple Gaussian distribution [43]–[45]. The inaccuracy may not affect significantly for the traffic flow analysis, for example, these models can reproduce real-world traffic phenomena like traffic oscillations and the fundamental diagram. However, it will cause significant evaluation biasedness on AV performance. In a few studies [44], the log-normal and extreme value distributions are applied. Although these distributions are more realistic than the Gaussian, the accuracy is still limited due to the model flexibility for fitting complicated driving behaviors in all situations using the same distribution.

Besides adding an external noise  $\epsilon(t)$ , the stochasticity can also be incorporated into model parameters  $\theta(t)$ . For example, Treiber et al. [40] proposed indifference regions in the form of action points to the model, so the new acceleration will be executed only when the change is greater than a threshold parameter, which follows a uniform distribution. Yang et al. [44] considered different human errors during car-following situations, where the length of time delay and distraction interval are modeled by exponential distribution and lognormal

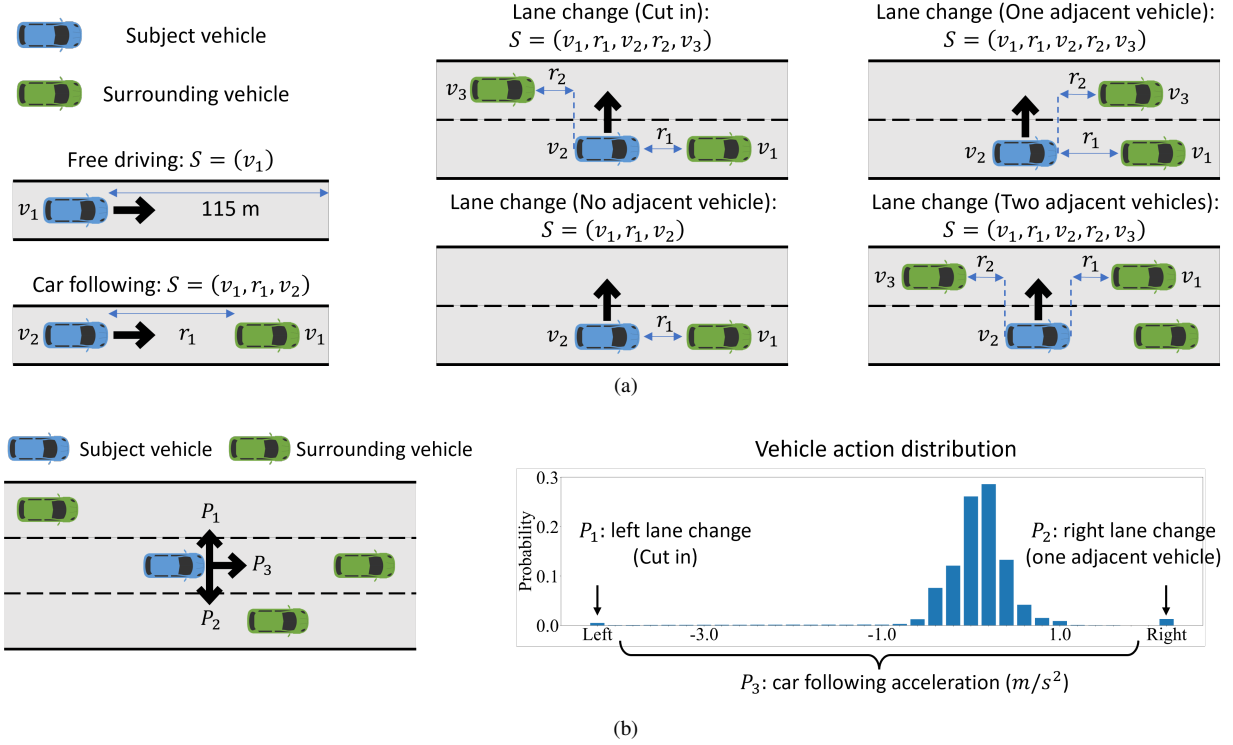


Fig. 3. Illustration of empirical behavior models: (a) longitudinal and lateral behavior models in this study, (b) illustration example of how to simulate a vehicle's action at a decision moment.

distribution according to real-world data, respectively. Game theory is applied in [46] to model stochastic lane-change behavior. Hamdar et al. [47], [48] proposed a utility-based stochastic car-following model where acceleration probability follows a continuous logit model. Again, these methods do not concern with the distributional accuracy of the driving behaviors after the stochasticity is introduced. There were two notable exceptions in [49], [50], the authors proposed stochastic car-following models to capture the distribution of time headway. They validate that the headway distribution of the simulation environment is consistent with the real world. However, only car-following behavior is considered in these studies, so they can only simulate the single-lane road. More importantly, the error accumulation issue has not been considered, which could severely distort the distribution for long-term simulation of NDE. More related studies can be found in [51]–[53] and references therein.

Notwithstanding the related studies, most existing methods cannot capture the accurate distribution of stochastic human driving behaviors. Therefore, the driving environment that is generated by these behavior models cannot accurately reproduce simulation environment statistics, which is critical for AV testing.

### III. DATA-DRIVEN NDE MODELING

In this section, we propose a simple yet effective data-driven method for NDE modeling leveraging large-scale NDD. Specifically, six empirical behavior models are constructed including free-driving, car-following, and four lane-changing behaviors with different driving conditions, and then the NDE

can be generated by combining the six empirical behavior models according to the driving condition at each time step (Section III-A). To construct each empirical behavior model, the large-scale NDD is processed and utilized in Section III-B. Then, a multi-lane highway driving environment is simulated to evaluate the performance of the empirical behavior models in Section III-C, which validates the data-driven method and further motivates the robust modeling step in Section IV.

#### A. Empirical behavior models

To construct the NDE, both longitudinal and lateral behaviors of human drivers need to be modeled based on the vehicle's own state and its surrounding situations  $S$ . For example, human drivers need to decide their longitudinal accelerations and decide whether to take a lateral lane-change maneuver. In this study, six behavior models are proposed including free-driving, car-following, and four lane-changing behaviors with different driving conditions, as shown in Fig. 3a. Specifically, the vehicle acceleration in the free-driving case is modeled that depends only on its current velocity, while the acceleration in the car-following case is modeled that depends on the velocity, range (relative position), and range rate (relative speed) of the subject vehicle and its preceding vehicle. To capture the lane-changing probability in different conditions, four lane-changing models are proposed, which output the lane change probability of the subject vehicle at each moment. For example, in the cut-in lane change situation, the lane-changing probability depends on velocities and distances between the subject vehicle and the preceding vehicle in the current lane and the vehicle behind in the target lane. We note that more

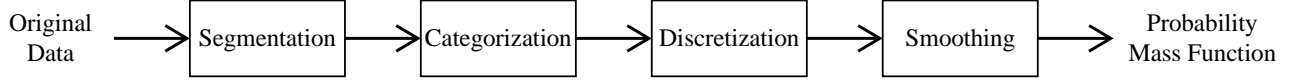


Fig. 4. Data processing flow chart.

lane-changing models could be constructed in this framework by dividing the driving conditions into more categories if needed.

After constructing the six behavior models, the NDE can be generated by combining the behavior models according to the driving condition at each time step. Taking Fig. 3b (left) as an example, the subject vehicle can take left lane change, keep car-following, or take right lane change at the moment. The left lane change behavior can be categorized as a cut-in behavior, where the lane-changing probability  $P_1$  can be obtained from the cut-in behavior model. The right lane change behavior can be categorized as a lane change with one adjacent vehicle, where the lane-changing probability  $P_2$  can also be obtained by the corresponding behavior model. Moreover, the longitudinal acceleration probability  $P_3$  can be obtained by the car-following behavior model. After normalization, we can obtain the action distribution of the vehicle as shown in Fig. 3b (right). Then, the subject vehicle's action will be sampled from this distribution and used to update its state to the next time step. To simplify the modeling process, longitudinal acceleration is assumed zero if the vehicle is making a lane change behavior. Also, if there is no vehicle in front, the ego-vehicle will not take lane-changing behavior. By repeating this process for all vehicles and time steps, the NDE can be generated.

The remaining question is how to construct the six behavior models with distributional accuracy. In this study, we propose to directly estimate empirical behavior distributions as the behavior models by leveraging large-scale NDD. As the NDD records all the information needed for the human driving behaviors, accurate empirical behavior models could be constructed if using sufficient amount of data with perfect quality. Although the actual data is usually limited by the data quality and quantity, these empirical behavior models could provide a good foundation and can be further improved as discussed in Section IV. Specifically, for each behavior model, we obtain the empirical probability  $P(a|S)$  for all the vehicle actions  $a \in \mathcal{A}$  at all discretized states  $S \in \mathcal{S}$ , where  $\mathcal{A}$  denotes the action space, and  $\mathcal{S}$  denotes the state space. Let  $F(S) = [P(a_1|S), \dots, P(a_{|\mathcal{A}|}|S)]$  denote the probability mass function under a certain state  $S$ , then the empirical behavior model can be denoted by

$$F = [F(S_1), \dots, F(S_{|\mathcal{S}|})] \in \mathbb{R}^{|\mathcal{S}| \times |\mathcal{A}|}. \quad (3)$$

Next, we will introduce how to process the NDD and construct  $F$  for all the six behavior models.

#### B. Naturalistic driving dataset processing

To construct empirical behavior models, we utilized large-scale NDD from the Integrated Vehicle Based Safety System

(IVBSS) dataset [54] and the Safety Pilot Model Deployment (SPMD) dataset [55] at the University of Michigan Transportation Research Institute (UMTRI). In the IVBSS program, 108 drivers ranging from 20 to 70 years old were recruited. Each participant drove the IVBSS vehicle equipped with the data acquisition system (DAS) for 6 weeks. The relative distance and speed with the leading vehicle are recorded by radar at 10 Hz. The SPMD program covered over 34.9 million travel miles and included 98 vehicles equipped with the DAS and Mobileye to record human naturalistic driving behaviors. The data were also recorded at 10 Hz with positions, speeds, and accelerations of ego-vehicles, relative speeds with surrounding vehicles, and both longitudinal and lateral distances between vehicles and lane markings. We queried partial datasets with the following criteria: (1) vehicle was traveling at a speed between 20 m/s and 40 m/s; (2) dry surface condition; (3) daylight condition. The resulting dataset includes approximately 8,200 driving hours data.

The data processing consists of four steps including segmentation, categorization, discretization, and smoothing, as shown in Fig. 4. Specifically, the original data were first segmented into trajectories and then categorized into specific groups based on the six driving situations defined in empirical behavior models. Then, a smoothing technique was applied to the discretized action distribution and finally, we could obtain the probability mass functions for each group, which constituted the six empirical behavior models. More details of the data processing steps can be found in Appendix. A. Fig. 5 demonstrates examples of constructed empirical behavior models. Specifically, Fig. 5a and Fig. 5b show examples of the vehicle longitudinal acceleration distributions in free-driving and car-following situations, respectively. For the car-following case, Fig. 5b indicates acceleration distribution when the ego-vehicle and its preceding vehicle have the same speed and their range is 30 meters. We can find that for both free-driving and car-following cases, the mean of acceleration is around zero, which is consistent with the intuition. Compared with the car-following situation, the probability of acceleration greater than zero is generally higher in the free-driving case, which is reasonable as well.

#### C. Performance evaluation of empirical behavior models

In this subsection, the performance of the NDE constructed by the six empirical behavior models is evaluated in a three-lane highway simulation, as illustrated in Fig. 3b (left). The detailed simulation settings can be found in Appendix. B. The Hellinger distance [56] is used to quantitatively measure the dissimilarity between the simulated distribution and the true distribution. The Hellinger distance ranges from 0 to

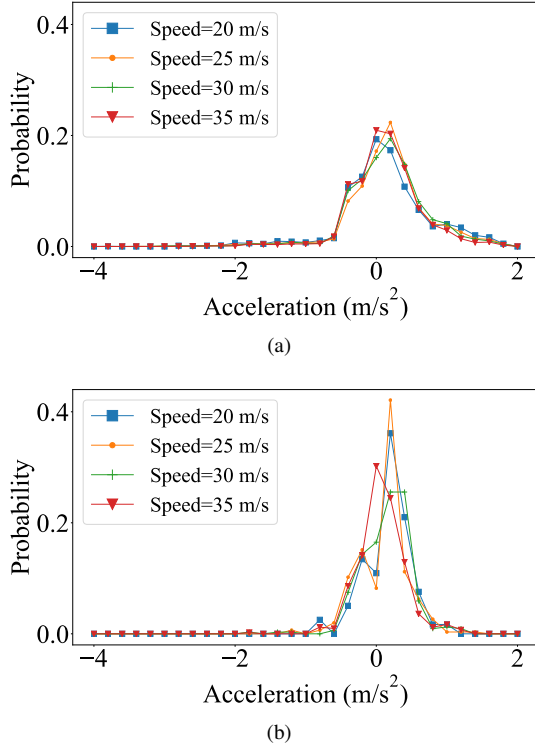


Fig. 5. Examples of empirical behavior models: (a) Free driving, (b) Car following ( $r_1 = 30$  m,  $v_1 = v_2$ ).

1, and the smaller the measurement, the better the model performance. To demonstrate the performance, the background vehicles velocity and range distributions, which are important for the AV testing, are investigated as shown in Fig. 6. Results show that although the distributions can roughly capture the trends of the real-world distributions, there still exist significant distributional inconsistency, particularly for the vehicle velocity. This inconsistency is caused by the error accumulation of the empirical behavior models, where the small model errors caused by the limited data quality and quantity are accumulated and amplified along with the simulation steps, as illustrated in Fig. 1. To address this issue, the robust NDE modeling step is developed in the next section to further improve the empirical models.

#### IV. ROBUST NDE MODELING

In this section, the robust NDE modeling step is proposed to refine empirical behavior models to minimize the accumulated errors using optimization methods. To achieve this goal, the key is to model the long-term effects of the error accumulation. Specifically, by modeling the vehicle state evolution as a Markov chain, the long-term effects of the error accumulation can be characterized by the stationary distribution of the Markov chain. Then, an optimization problem is formulated to minimize the accumulated errors by adjusting the empirical behavior models, which results in the NDE model with more accurate distributions. In the following paragraphs, we first propose the optimization framework in Section IV-A and then apply the framework on the longitudinal behavior models in Section IV-B.

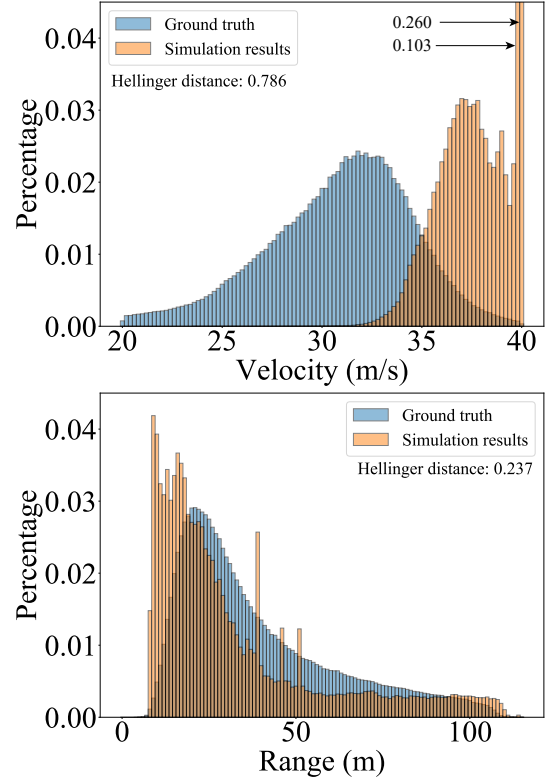


Fig. 6. Velocity and range distributions of the NDE using empirical behavior models.

##### A. Optimization framework

In order to solve the error accumulation problem, we need to measure the accumulated error of the NDE generated by the empirical behavior models. One possible way is to simulate the NDE, collect the data, and obtain the simulated NDE distribution. However, the computational burden of this method is very heavy since a large number of simulations are needed to obtain an accurate estimation. To overcome this problem, we propose to measure the NDE distribution by analyzing the stationary distribution of the NDE Markov chain. By using this analytical method, the NDE stationary distribution serves as an accurate approximation of the simulated environment, which reflects the performance of the empirical behavior models. By fitting the simulated stationary distribution with real-world ground-truth, we can improve the NDE accuracy and solve the error accumulation issue.

Following this idea, the optimization framework can be formulated as in Fig. 7. The decision variable is the vehicle behavior model  $F$  as shown in Eq. (3), and the objective is to minimize the adjustment to the empirical behavior model  $F^*$  while ensuring the accuracy of the stationary distribution. To achieve this objective, there are generally four sets of constraints in the optimization formulation. The first set of constraints is the standard definition of stationary distribution, which indicate that the state will always follow its stationary distribution after reaching the steady state. The second set of constraints describes the relationship between the behavior model and Markov chain state transition probability. The stochastic vehicle behavior model outputs actions for the



next time step and therefore determines the state transition process. The third set of constraints is to match the stationary distribution of the simulation with the real-world ground-truth distribution, which is the key to reducing the accumulated errors. As a result, the simulated environment can be guaranteed to fit the desired real-world statistics (e.g., velocity and range distributions) even after a long simulation time horizon. The last set of constraints denotes other standard requirements, such as non-negative constraints of probability mass functions, normalization of stationary distribution, etc.

$$\begin{aligned}
 & \min_F \quad \text{distance}(F, F^*) \\
 \text{s.t.} \quad & 1. \text{ Definition of the stationary distribution.} \\
 & 2. \text{ Relation between behavior model and Markov} \\
 & \quad \text{chain transition probability.} \\
 & 3. \text{ Relation between stationary distribution and} \\
 & \quad \text{ground-truth distribution.} \\
 & 4. \text{ Other constraints.}
 \end{aligned}$$

Fig. 7. Overall formulation of the proposed robust modeling step.

### B. Optimization of longitudinal behavior models

In this section, we apply the proposed framework to optimize the two empirical longitudinal behavior models as a proof of concept, while keeping the four empirical lateral behavior models unchanged. As the velocities cannot be well modeled by the empirical models as shown in Fig. 6, we choose the velocity distribution as the optimization target.

For the free-driving behavior model, we define the discretized speed as the state of the Markov chain. It is easy to find that the Markov chain is finite, irreducible, and aperiodic, so there exists a unique positive stationary distribution  $\pi$  [57] satisfying

$$\pi^T \mathbf{P} = \pi^T, \quad (4)$$

$$\sum_{S \in \mathcal{S}} \pi_S = 1, \quad (5)$$

$$\pi \succcurlyeq 0, \quad (6)$$

where  $\mathbf{P}$  is the state transition probability matrix. As the vehicle longitudinal acceleration depends only on its current speed in the free-driving situation, the state transition probability matrix  $\mathbf{P}$  is essentially a function of the behavior model  $F$  in Eq. (3) as

$$\mathbf{P}(S_i, S_j) = G(F), \forall S_i, S_j \in \mathcal{S}, \quad (7)$$

where  $G(\cdot)$  is a linear mapping from the longitudinal acceleration to the state transition. For example, if the current speed falls in the state  $S_i$ , the next speed after the transition is  $S_j$ , the time resolution is  $\Delta t$ , and the probability of taking acceleration  $a$  that satisfies the  $S_j = S_i + a \cdot \Delta t$  is  $p(a|S_i)$ , then  $\mathbf{P}(S_i, S_j) = p(a|S_i)$ . Moreover, as the goal

of the optimization is to match the vehicle stationary speed distribution with the real-world speed distribution in the free-driving situation, we have

$$\pi = \pi^*, \quad (8)$$

where  $\pi^*$  is the ground-truth of the speed distribution in free-driving situations that is obtained from the large-scale NDD.

Finally, the optimization problem can be formulated as below:

$$\min_F \quad \|F - F^*\|_{Frob} \quad (9)$$

$$\text{s.t.} \quad \pi^T \mathbf{P} = \pi^T, \quad (10)$$

$$G(F) = \mathbf{P}(S_i, S_j), \forall S_i, S_j \in \mathcal{S}, \quad (11)$$

$$\pi = \pi^*, \quad (12)$$

$$\sum_{a \in \mathcal{A}} F(a|S) = 1, \forall S \in \mathcal{S}, \quad (13)$$

$$\sum_{S_j \in \mathcal{S}} \mathbf{P}(S_i, S_j) = 1, \forall S_i \in \mathcal{S}, \quad (14)$$

$$\sum_{S \in \mathcal{S}} \pi_S = 1, \quad (15)$$

$$F, \mathbf{P}, \pi \succcurlyeq 0. \quad (16)$$

The Frobenius norm  $\|\cdot\|_{Frob}$  is adopted to measure the distance between the optimized free-driving model  $F$  and empirical free-driving model  $F^*$ . Comparing with the constraints discussed in Fig. 7, Eq. (10) denotes the definition of the stationary distribution, Eq. (11) denotes the relation between behavior model and transition probability, Eq. (12) denotes the distributional consistency between the stationary distribution and the ground-truth, and Eqs. (13-16) denote other constraints including the normalization requirements for the acceleration probability mass function, state transition probability matrix, and stationary distribution, respectively, and the non-negative requirements. It can be found out that this is a linear programming problem that can be solved efficiently using commercial solvers, for example, Gurobi [58].

For the car-following situation, the vehicle state is composed of the speed of the subject vehicle ( $v$ ), range ( $r$ ), and range rate ( $rr$ ) with the preceding vehicle. The state transition in the car-following situation depends not only on the subject vehicle action but also preceding vehicle action, which makes the optimization problem more complex. To solve this issue, we optimize the steady-state situation of the car-following model, which is a necessary condition regardless of the evolving process to the stationary distribution. As the preceding vehicle has reached the steady-state, the ego-vehicle state transition relies only upon its own action. Then, the optimization problem can be formulated as the same as Eqs. (9-16), where decision variables are the probability mass functions of the car-following accelerations ( $F$  in Eq. (3)), and Eq. (10) is a three-dimensional joint state distribution (i.e.,  $v$ ,  $r$ , and  $rr$ ). It is also a linear programming problem that can be solved efficiently.

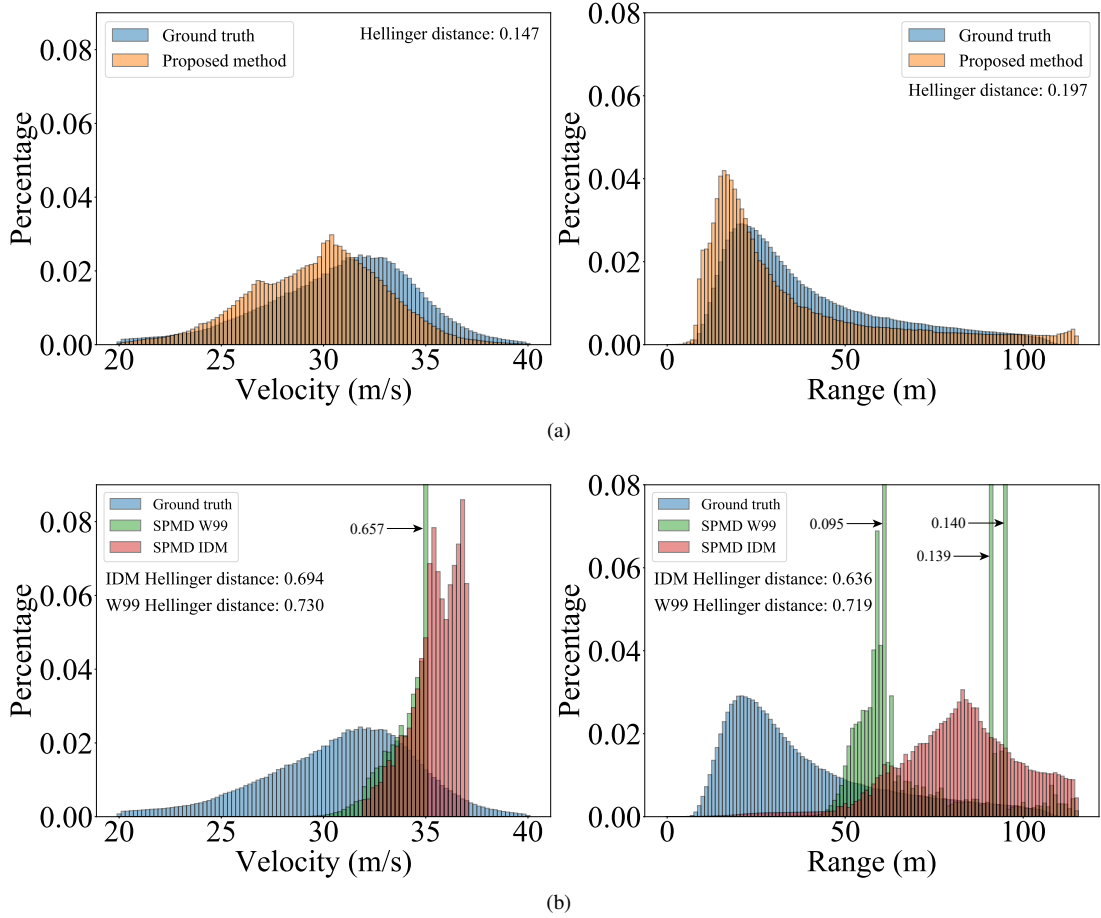


Fig. 8. Velocity and range distributions of the: (a) proposed method; (b) SUMO simulator.

## V. PERFORMANCE EVALUATION

In this section, the performance of the proposed NDE modeling framework is evaluated.

### A. Distributional consistency

As the distributional consistency is critical for the generated NDE, we first evaluate whether the proposed NDE can generate accurate velocity and range distributions, compared with the existing NDE baseline (i.e., SUMO [59]) and the empirical models constructed in Section III. Specifically, two existing car-following models, the IDM [21] and the Wiedemann 99 model [60], and SUMO LC2013 lane-changing model [61] are selected as the existing NDE baseline, which are widely applied in existing traffic simulators. For fair comparisons, the model parameters are calibrated with the SPMD NDD described in Section III-B using the calibration method developed in [62], [63]. More simulation settings can be found in Appendix. B.

Fig. 8 shows the results of the proposed NDE model and existing NDE models. It can be found that the proposed NDE model can significantly better reproduce the real-world velocity and range distributions than existing ones. Specifically, both the IDM and Wiedemann 99 models are concentrated in a small interval of velocity and range, while the real-world distributions range among a much wider interval. It is

reasonable as these existing models are designed for accident-free purposes and therefore might be more conservative and deterministic. Besides using model parameters calibrated in this study, we also examine the performance using model parameters provided from the literature, where similar results are obtained (see Appendix. D for more details).

Compared with the results before the optimization as shown in Fig. 6, the accuracy of the simulated velocity distribution is also significantly improved, which validates the effectiveness of the robust modeling step. To further quantify the performance improvement, the Hellinger distances of all these models are calculated as listed in Table. I. Results show that the empirical behavior models can achieve a better performance than the existing NDE models (similar performance in velocity but significantly better performance in range), and the optimized models can achieve the best performance. These results validate the effectiveness of both the data-driven and optimization steps and show that the proposed method can generate the NDE consistent with the real-world driving environment.

In addition to the velocity and range distributions, we also calculated the lane-changing statistic of the proposed NDE to further examine its lateral behavior performance. From the simulation results, the average travel distance for one lane change is 4.86 kilometers. In the real-world driving environment, the same statistic is 4.45 kilometers per lane



TABLE I  
QUANTITATIVE PERFORMANCE EVALUATION FOR DIFFERENT METHODS.

Method \ Metric	Velocity	Range
Empirical behavior models	0.786	0.237
SUMO (SPMD IDM)	0.755	0.659
SUMO (SPMD W99)	0.629	0.691
Proposed method	<b>0.147</b>	<b>0.197</b>

change on the highway [64]. Therefore, the proposed NDE can also reproduce a reasonable number of lane changes as in the real-world driving environment, which can further demonstrate the fidelity of the proposed NDE.

### B. AV testing using the proposed NDE

To further demonstrate the capability of the proposed NDE model for AV testing, we test the safety performance of an AV model utilizing the proposed NDE and SUMO (SPMD IDM) environments, respectively. Following previous studies on AV testing [2], [7], [8], [13], the AV accident rate in the NDE is chosen as the measurement, and the Monte Carlo method is applied to estimate the accident rate as shown in Eq. (1). Specifically, the IDM and MOBIL models [13] are used as the AV model, one simulation test is conducted for a constant driving distance (400 m) of the AV, and the testing result (accident or not) of each simulation is utilized to calculate the accident rate. To obtain accurate evaluation results, the AV will run  $5 \times 10^6$  simulations in the proposed NDE and SUMO environments, respectively, which is approximately 1.2 million driving miles for the AV under test. The experiments take around four hours using the University of Michigan's Great Lakes High-Performance Computing cluster with 1,300 cores (Intel Xeon Gold 6154 processor) and 9,000 GB RAM.

During the simulation tests in the SUMO environment, there is no accident occurred so the estimated AV accident rate is zero. This is because the SUMO environment is designed for accident-free simulations, and therefore, it cannot effectively evaluate the AV safety performance. During the simulation tests in the proposed NDE, however, the estimated accident rate of the AV is  $5.5 \times 10^{-5}$  accidents per simulation, where 276 accidents are generated in the AV testing process. The estimation results with the number of tests can be found in Fig. 9a, where the shaded area denotes the 90% confidence interval, and the accident type distribution is shown in Fig. 9b based on the definitions of the National Highway Traffic Safety Administration [65]. The results show that the proposed NDE can successfully generate diverse safety-critical situations to evaluate the AV safety performance. With more distributionally accurate NDE models, the safety performance of AVs could be evaluated more effectively.

## VI. CONCLUSIONS

In this paper, we propose a distributionally consistent NDE modeling framework for AV testing purposes. We first propose

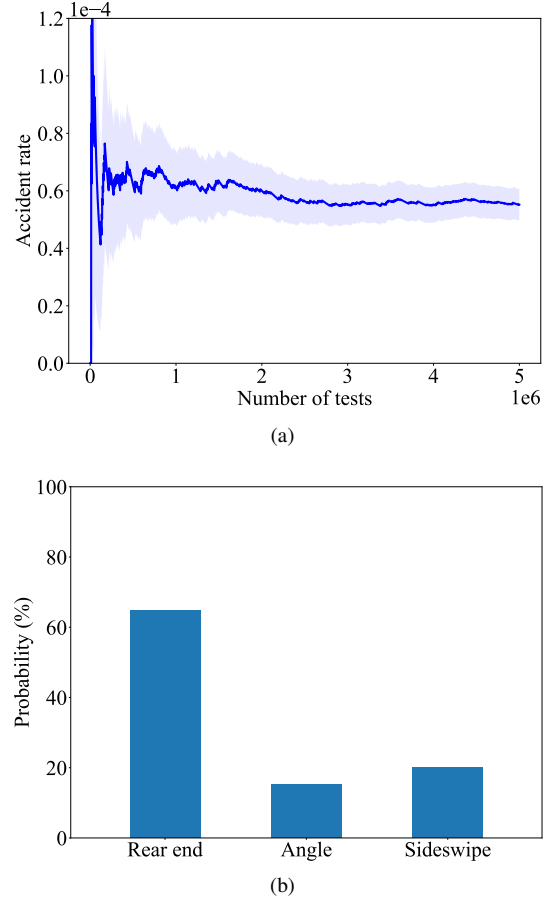


Fig. 9. AV testing and evaluation results using the proposed NDE: (a) estimation results of the accident rate (shaded area denotes the 90% confidence interval), (b) accident type distribution.

to directly generate empirical behavior models using large-scale NDD. These empirical behavior models can serve as basic models since they will converge in probability to the real behavior models when the data size and quality are sufficiently large and accurate. To address the error accumulation issue and guarantee the accuracy of the NDE throughout the simulation, a robust modeling step based on the Markov process is proposed, which optimizes the empirical models by matching simulated stationary distributions with the ground truth. The proposed method is validated for the multilane highway driving environment using large-scale real-world NDD. The vehicle speed and range distributions generated by the proposed NDE are consistent with the empirical ground truth, which are important for AV testing, and the lane-changing statistic is also examined to be consistent with the ground truth. Moreover, the generated NDE is utilized to test the safety performance of an AV agent, which further validates the effectiveness of the proposed NDE.

There are certain limitations in the current work that can be addressed by future research. For example, homogeneous vehicles are considered in this study where all background vehicles share the same behavior models and vehicle classes. In the real-world driving environment, there are different vehicle classes, such as sedan, truck, heavy vehicle, etc. Moreover, within a specific vehicle class, they may have

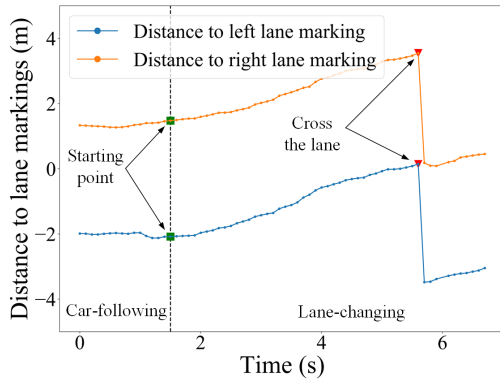


Fig. 10. Lane-changing events identification example: the subject vehicle is doing a left lane change.

different behavior models, for example, some drivers are more aggressive, and some drivers are more conservative. We leave these for future research.

## APPENDIX A

### NATURALISTIC DRIVING DATA PROCESSING

First, the original data were segmented into trajectories with the following requirements: (1) the time should be continuous and does not have discontinuity of more than 2 seconds, (2) the identification of the surrounding vehicles is consistent throughout the trajectory, (3) each trajectory should last more than 3 seconds. Data that are too noisy (with severe speed and/or position oscillations) are discarded.

Second, considering the driving environment of the subject vehicle, trajectory data points will be categorized into the six situations as illustrated in Fig. 3a, correspondingly. An important step in the categorization is to identify the lane-changing event by analyzing the lateral distance to the lane markings. Fig. 10 shows an example that the ego-vehicle is doing a left lane change. Note that the sign of the distance to lane marking differentiates the left and right lane markings. Fig. 10 shows the whole process of a left lane-changing event: the vehicle is approaching the left lane marking and cross the lane when the distance to the left lane marking equals zero, and then change to the maximum (lane width) after entering the target lane. The starting moment and crossing the lane moment of lane-changing events can be identified based on both the distance and slope change of the distance, accordingly. Similar techniques are also utilized for lane-changing detection in a recent study [66]. The starting point of the lane-changing event will be used for calculating the lane change probability.

Third, for each data point, the state was discretized using the following resolutions: except for the speed resolution of longitudinal behavior is 0.2 m/s, the speed and spacing resolutions are 1 m/s and 1 m for all other situations. The longitudinal acceleration discretization resolution is set as 0.2  $m/s^2$ . Therefore, at each decision moment, a vehicle has 33 possible actions: left lane change, 31 longitudinal accelerations (range from -4 to 2  $m/s^2$  with 0.2 as the discretization resolution), right lane change.

Finally, the Moving Average (MA) [67] smoothing technique was applied. During the smoothing process, states

leading to an inevitable crash will not be included. After that, the empirical probability of each action at each state can be calculated by its frequency in the dataset of the corresponding category. These constitute empirical data-driven vehicle behavior models.

## APPENDIX B

### EXPERIMENT SETTINGS

The experiment settings of the proposed method and the SUMO baseline is discussed in the section. For the proposed method, a three-lane highway driving environment is developed based on an open-source highway traffic simulator [68]. The bicycle model is implemented to update vehicle states at a 10Hz frequency. All lane-changing maneuvers are set completed in 1 second. To be consistent with the NDD, the speed of the NDE simulation is bounded between 20 to 40 m/s, and the longitudinal acceleration is bounded between -4 to 2  $m/s^2$ . Since both the longitudinal and lateral models are data-driven, there are inevitably states where no NDD is collected. We will use the IDM and MOBIL model for states not covered by the proposed behavior models. The IDM model parameters are calibrated from the same NDD. The MOBIL model parameters are partially from [69] which are also calibrated using the SPMD dataset. The detailed model parameters are listed in the next paragraph. The simulation initialization method determines the initial state of all vehicles, which includes the position and speed, etc. A realistic initialization is preferred to shorten the required warm-up time, which can improve the simulation efficiency. In this study, a data-driven initialization method is proposed based on NDD and the details can be found in Appendix. C. Using the proposed initialization method, around 60 vehicles will be initialized for each simulation. It is approximately 1360 vehicles/hour/lane, which belongs to level of service (LOS) C for multilane highways [70]. We ran 100 simulations to mitigate the randomness effect. To fully examine the error accumulation issue, each simulation ran 15 minutes, which includes 10 minutes of warm-up time and 5 minutes of data collection.

The calibrated parameters of the IDM model using the SPMD are: maximum acceleration (0.8  $m/s^2$ ), desired speed (37 m/s), exponent parameter (3.0), comfortable deceleration (-1.3  $m/s^2$ ), gap at standstill (0.1 m), and desired time headway (0.8 s). To generate a stochastic version IDM, the output acceleration will follow a Gaussian distribution with the original output acceleration as mean and 0.3 as standard deviation. The parameters of the MOBIL model are: politeness factor (0.1), utility threshold (0.2  $m/s^2$ ), and maximum safe deceleration (-3  $m/s^2$ ).

For the SUMO baseline, all simulation settings are the same as the proposed method. Each simulation lasts for 15 minutes, which includes 10 minutes of warm-up time and 5 minutes of data collection. We set the input traffic flow as 1360 vehicles/hour/lane and 60 vehicles will be generated in each simulation. The initial speed of the vehicle is set as 32 m/s based on NDD. To account for the stochasticity of the simulator, we ran 100 simulations for each model to collect data.

## APPENDIX C

### THE PROPOSED DATA-DRIVEN SIMULATION INITIALIZATION METHOD

We propose a data-driven initialization method to sequentially determine the  $(i + 1)$ -th vehicle state  $(x_i, y_i, v_i)$ , i.e., longitudinal position, lateral position, and velocity, of downstream vehicles based on its upstream  $i$ -th vehicles' states. The lateral position  $y_i$  is the same as the lateral coordinates of its lane center. The first vehicle of each lane is determined by sampling its longitudinal position inside an initial zone from a uniform distribution and its velocity from the empirical velocity distribution. This can be expressed as

$$x_i \sim U(0, d_0), \quad (17)$$

$$v_i \sim \pi_v^*, \quad (18)$$

where  $U(\cdot, \cdot)$  denotes the uniform distribution,  $d_0$  is the predetermined initial zone size,  $v_0$  is the speed, and  $\pi_v^*$  is the empirical velocity distribution obtained from the NDD. Based on the state of the  $i$ -th vehicle, we can determine its downstream  $(i + 1)$ -th vehicle state. An indicator variable follows a Bernoulli distribution  $I_i \sim B(p_{CF})$  is sampled to determine whether the  $i$ -th vehicle is in the car-following ( $I_i = 1$ ) situation or free-driving ( $I_i = 0$ ) situation.  $p_{CF}$  is the probability a vehicle is in the car-following case, which can be approximated from NDD. Then the joint distribution of range  $r$  and range rate  $rr$  given the current speed  $g(r, rr|v_i)$  is queried from the NDD if  $I_i = 1$ . Then, the position and velocity of the next (downstream) vehicle can be obtained by

$$x_{i+1} = x_i + r, \quad (19)$$

$$y_{i+1} = y_i, \quad (20)$$

$$v_{i+1} = v_i + rr, \quad (21)$$

where  $r, rr$  is the range and range rate sampled from  $g(r, rr|v_i)$ , and the lateral position of the  $(i + 1)$ -th vehicle is the same as the  $i$ -th vehicle since they are in the same lane. If  $I_i = 0$ , the next vehicle is randomly generated in a new initial zone outside the car-following observation range, and the velocity follows the empirical velocity distribution. It can be represented as

$$x_{i+1} = x_i + d_{obs} + r, \quad (22)$$

$$r \sim U(0, d_0), \quad (23)$$

$$y_{i+1} = y_i, \quad (24)$$

$$v_{i+1} \sim \pi_v^*, \quad (25)$$

where  $d_{obs}$  is the predetermined car-following observation range suggested by the NDD. Vehicles on each lane can be sequentially generated by repeating this process. Note that unrealistic initialization that leads to trivial initial collision will be rejected and resampled. Based on the data, the parameters used in the study are  $d_0 = 50m$ ,  $p_{CF} = 0.68$ , and  $d_{obs} = 115m$ .

## APPENDIX D

### PERFORMANCE OF BASELINE METHODS USING PARAMETERS FROM THE LITERATURE

Besides using parameters calibrated by ourselves, we also use model parameters from the literature to fully illustrate the performance of existing methods which includes those calibrated by the NDD from Virginia, US [29] (denoted as VT100 IDM), and Shanghai, China [31] (denoted as Shanghai IDM and Shanghai W99). The vehicle initial speed is set based on the parameters of each model, which is 26 m/s for VT100 IDM, 28 m/s for Shanghai IDM, and 22 m/s for Shanghai W99. Other simulation settings are the same as discussed in Appendix. B., where each model runs 20 simulations to collect data. The results are shown in Fig. 11. Although the NDD reported in Fig. 11 is not the same one used for calibration in the literature, the comparison is still informative. The distributions generated using existing methods are concentrated in relatively dense regions, however, the real-world distribution spreads naturally among the whole intervals.

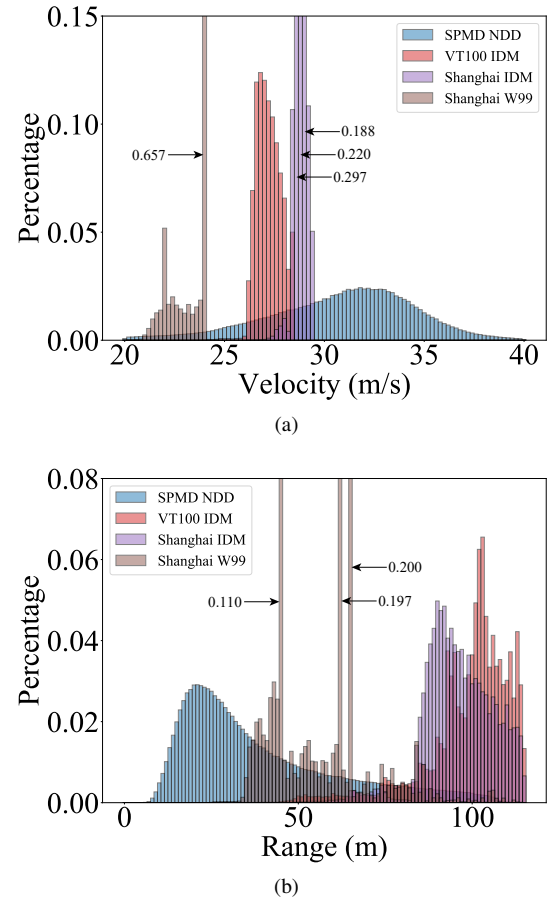


Fig. 11. Velocity and range distributions that generated using model parameters from the literature.

## ACKNOWLEDGMENT

The authors would like to thank Dr. Bo Yu for his help in the data querying process.

## REFERENCES

- [1] N. Kalra and S. M. Paddock, "Driving to safety: How many miles of driving would it take to demonstrate autonomous vehicle reliability?" *Transportation Research Part A: Policy and Practice*, vol. 94, pp. 182–193, 2016.
- [2] D. Zhao, H. Lam, H. Peng, S. Bao, D. J. LeBlanc, K. Nobukawa, and C. S. Pan, "Accelerated evaluation of automated vehicles safety in lane-change scenarios based on importance sampling techniques," *IEEE transactions on intelligent transportation systems*, vol. 18, no. 3, pp. 595–607, 2016.
- [3] H. Hungar, F. Köster, and J. Mazzega, "Test specifications for highly automated driving functions: Highway pilot," 2017.
- [4] M. Koren, S. Alsaif, R. Lee, and M. J. Kochenderfer, "Adaptive stress testing for autonomous vehicles," in *2018 IEEE Intelligent Vehicles Symposium (IV)*. IEEE, 2018, pp. 1–7.
- [5] M. O'Kelly, A. Sinha, H. Namkoong, R. Tedrake, and J. C. Duchi, "Scalable end-to-end autonomous vehicle testing via rare-event simulation," *Advances in Neural Information Processing Systems*, vol. 31, pp. 9827–9838, 2018.
- [6] L. Li, X. Wang, K. Wang, Y. Lin, J. Xin, L. Chen, L. Xu, B. Tian, Y. Ai, J. Wang, D. Cao, Y. Liu, C. Wang, N. Zheng, and F.-Y. Wang, "Parallel testing of vehicle intelligence via virtual-real interaction," *Science Robotics*, 2019.
- [7] S. Feng, Y. Feng, C. Yu, Y. Zhang, and H. X. Liu, "Testing scenario library generation for connected and automated vehicles, part I: Methodology," *IEEE Transactions on Intelligent Transportation Systems*, 2020.
- [8] S. Feng, Y. Feng, H. Sun, S. Bao, Y. Zhang, and H. X. Liu, "Testing scenario library generation for connected and automated vehicles, part II: Case studies," *IEEE Transactions on Intelligent Transportation Systems*, 2020.
- [9] S. Feng, Y. Feng, H. Sun, Y. Zhang, and H. X. Liu, "Testing scenario library generation for connected and automated vehicles: An adaptive framework," *IEEE Transactions on Intelligent Transportation Systems*, 2020.
- [10] S. Feng, Y. Feng, X. Yan, S. Shen, S. Xu, and H. X. Liu, "Safety assessment of highly automated driving systems in test tracks: a new framework," *Accident Analysis & Prevention*, vol. 144, p. 105664, 2020.
- [11] M. Klischat and M. Althoff, "Synthesizing traffic scenarios from formal specifications for testing automated vehicles," in *Proc. of the IEEE Intelligent Vehicles Symposium*, 2020.
- [12] L. Waymo, "Waymo safety report," <https://storage.googleapis.com/sdc-prod/v1/safety-report/2020-09-waymo-safety-report.pdf>, 2020.
- [13] S. Feng, X. Yan, H. Sun, Y. Feng, and H. X. Liu, "Intelligent driving intelligence test for autonomous vehicles with naturalistic and adversarial environment," *Nature communications*, vol. 12, no. 1, pp. 1–14, 2021.
- [14] H. Sun, S. Feng, X. Yan, and H. X. Liu, "Corner case generation and analysis for safety assessment of autonomous vehicles," *Transportation research record*, vol. 2675, no. 11, pp. 587–600, 2021.
- [15] W. Li, C. Pan, R. Zhang, J. Ren, Y. Ma, J. Fang, F. Yan, Q. Geng, X. Huang, H. Gong *et al.*, "AADS: Augmented autonomous driving simulation using data-driven algorithms," *Science Robotics*, 2019.
- [16] X. B. Peng, M. Andrychowicz, W. Zaremba, and P. Abbeel, "Sim-to-real transfer of robotic control with dynamics randomization," in *2018 IEEE international conference on robotics and automation (ICRA)*. IEEE, 2018, pp. 3803–3810.
- [17] S. James, P. Wohlhart, M. Kalakrishnan, D. Kalashnikov, A. Irpan, J. Ibarz, S. Levine, R. Hadsell, and K. Bousmalis, "Sim-to-real via sim-to-sim: Data-efficient robotic grasping via randomized-to-canonical adaptation networks," in *Proceedings of the IEEE/CVF Conference on Computer Vision and Pattern Recognition*, 2019, pp. 12 627–12 637.
- [18] W. Zhao, J. P. Queralta, and T. Westerlund, "Sim-to-real transfer in deep reinforcement learning for robotics: a survey," in *2020 IEEE Symposium Series on Computational Intelligence (SSCI)*. IEEE, 2020, pp. 737–744.
- [19] S. Manivasagam, S. Wang, K. Wong, W. Zeng, M. Sazanovich, S. Tan, B. Yang, W.-C. Ma, and R. Urtasun, "Lidarsim: Realistic lidar simulation by leveraging the real world," in *Proceedings of the IEEE/CVF Conference on Computer Vision and Pattern Recognition*, 2020, pp. 11 167–11 176.
- [20] Y. Chen, F. Rong, S. Duggal, S. Wang, X. Yan, S. Manivasagam, S. Xue, E. Yumer, and R. Urtasun, "Geosim: Realistic video simulation via geometry-aware composition for self-driving," in *Proceedings of the IEEE/CVF Conference on Computer Vision and Pattern Recognition*, 2021, pp. 7230–7240.
- [21] M. Treiber, A. Hennecke, and D. Helbing, "Congested traffic states in empirical observations and microscopic simulations," *Physical review E*, vol. 62, no. 2, p. 1805, 2000.
- [22] A. Kesting, M. Treiber, and D. Helbing, "General lane-changing model MOBIL for car-following models," *Transportation Research Record*, vol. 1999, no. 1, pp. 86–94, 2007.
- [23] A. B. Owen, *Monte Carlo theory, methods and examples*, 2013.
- [24] L. Waymo, "Simulation city: Introducing waymo's most advanced simulation system yet for autonomous driving," <https://blog.waymo.com/2021/06/SimulationCity.html>, 2021.
- [25] R. Wiedemann, "Simulation des strassenverkehrsflusses," 1974, in: *Proceedings of the Schriftenreihe des instituts fir Verkehrswesen der Universitiit Karlsruhe, Germany*.
- [26] P. G. Gipps, "A behavioural car-following model for computer simulation," *Transportation Research Part B: Methodological*, vol. 15, no. 2, pp. 105–111, 1981.
- [27] P. Gipps, "A model for the structure of lane-changing decisions," *Transportation Research Part B: Methodological*, vol. 20, no. 5, pp. 403–414, 1986.
- [28] V. Punzo, B. Ciuffo, and M. Montanino, "Can results of car-following model calibration based on trajectory data be trusted?" *Transportation research record*, vol. 2315, no. 1, pp. 11–24, 2012.
- [29] J. Sangster, H. Rakha, and J. Du, "Application of naturalistic driving data to modeling of driver car-following behavior," *Transportation research record*, vol. 2390, no. 1, pp. 20–33, 2013.
- [30] L. Li, X. M. Chen, and L. Zhang, "A global optimization algorithm for trajectory data based car-following model calibration," *Transportation Research Part C: Emerging Technologies*, vol. 68, pp. 311–332, 2016.
- [31] M. Zhu, X. Wang, A. Tarko *et al.*, "Modeling car-following behavior on urban expressways in shanghai: A naturalistic driving study," *Transportation research part C: emerging technologies*, vol. 93, pp. 425–445, 2018.
- [32] C. Osorio and V. Punzo, "Efficient calibration of microscopic car-following models for large-scale stochastic network simulators," *Transportation Research Part B: Methodological*, vol. 119, pp. 156–173, 2019.
- [33] X. Wang, R. Jiang, L. Li, Y. Lin, X. Zheng, and F.-Y. Wang, "Capturing car-following behaviors by deep learning," *IEEE Transactions on Intelligent Transportation Systems*, vol. 19, no. 3, pp. 910–920, 2017.
- [34] X. Huang, J. Sun, and J. Sun, "A car-following model considering asymmetric driving behavior based on long short-term memory neural networks," *Transportation research part C: emerging technologies*, vol. 95, pp. 346–362, 2018.
- [35] M. Zhu, X. Wang, and Y. Wang, "Human-like autonomous car-following model with deep reinforcement learning," *Transportation research part C: emerging technologies*, vol. 97, pp. 348–368, 2018.
- [36] X. Zhang, J. Sun, X. Qi, and J. Sun, "Simultaneous modeling of car-following and lane-changing behaviors using deep learning," *Transportation research part C: emerging technologies*, vol. 104, pp. 287–304, 2019.
- [37] D.-F. Xie, Z.-Z. Fang, B. Jia, and Z. He, "A data-driven lane-changing model based on deep learning," *Transportation research part C: emerging technologies*, vol. 106, pp. 41–60, 2019.
- [38] J. A. Laval, C. S. Toth, and Y. Zhou, "A parsimonious model for the formation of oscillations in car-following models," *Transportation Research Part B: Methodological*, vol. 70, pp. 228–238, 2014.
- [39] Z. He, L. Zheng, and W. Guan, "A simple nonparametric car-following model driven by field data," *Transportation Research Part B: Methodological*, vol. 80, pp. 185–201, 2015.
- [40] M. Treiber and A. Kesting, "The intelligent driver model with stochasticity-new insights into traffic flow oscillations," *Transportation research procedia*, vol. 23, pp. 174–187, 2017.
- [41] A. Kuefler, J. Morton, T. Wheeler, and M. Kochenderfer, "Imitating driver behavior with generative adversarial networks," in *2017 IEEE Intelligent Vehicles Symposium (IV)*. IEEE, 2017, pp. 204–211.
- [42] R. Bhattacharyya, B. Wulfe, D. Phillips, A. Kuefler, J. Morton, R. Senanayake, and M. Kochenderfer, "Modeling human driving behavior through generative adversarial imitation learning," 2020.
- [43] H. Yeo, "Asymmetric microscopic driving behavior theory," Ph.D. dissertation, University of California, Berkeley, 2008.
- [44] H.-H. Yang and H. Peng, "Development of an errorable car-following driver model," *Vehicle System Dynamics*, vol. 48, no. 6, pp. 751–773, 2010.
- [45] L. Li and X. M. Chen, "Vehicle headway modeling and its inferences in macroscopic/microscopic traffic flow theory: A survey," *Transportation Research Part C: Emerging Technologies*, vol. 76, pp. 170–188, 2017.
- [46] A. Talebpour, H. S. Mahmassani, and S. H. Hamdar, "Modeling lane-changing behavior in a connected environment: A game theory approach," *Transportation Research Procedia*, vol. 7, pp. 420–440, 2015.

- [47] S. H. Hamdar, M. Treiber, H. S. Mahmassani, and A. Kesting, "Modeling driver behavior as sequential risk-taking task," *Transportation research record*, vol. 2088, no. 1, pp. 208–217, 2008.
- [48] S. H. Hamdar, H. S. Mahmassani, and M. Treiber, "From behavioral psychology to acceleration modeling: Calibration, validation, and exploration of drivers' cognitive and safety parameters in a risk-taking environment," *Transportation Research Part B: Methodological*, vol. 78, pp. 32–53, 2015.
- [49] F. Wang, L. Li, J.-M. Hu, Y. Ji, R. Ma, and R. Jiang, "A markov-process inspired ca model of highway traffic," *International Journal of Modern Physics C*, vol. 20, no. 01, pp. 117–131, 2009.
- [50] X. Chen, L. Li, and Y. Zhang, "A markov model for headway/spacing distribution of road traffic," *IEEE Transactions on Intelligent Transportation Systems*, vol. 11, no. 4, pp. 773–785, 2010.
- [51] Z. Zheng, "Recent developments and research needs in modeling lane changing," *Transportation research part B: methodological*, vol. 60, pp. 16–32, 2014.
- [52] M. Saifuzzaman and Z. Zheng, "Incorporating human-factors in car-following models: a review of recent developments and research needs," *Transportation research part C: emerging technologies*, vol. 48, pp. 379–403, 2014.
- [53] Q. Chao, H. Bi, W. Li, T. Mao, Z. Wang, M. C. Lin, and Z. Deng, "A survey on visual traffic simulation: Models, evaluations, and applications in autonomous driving," in *Computer Graphics Forum*, vol. 39, no. 1. Wiley Online Library, 2020, pp. 287–308.
- [54] J. Sayer, D. LeBlanc, S. Bogard, D. Funkhouser, S. Bao, M. L. Buonaros, A. Blankespoor *et al.*, "Integrated vehicle-based safety systems field operational test: Final program report," United States. Joint Program Office for Intelligent Transportation Systems, Tech. Rep., 2011.
- [55] D. Bezzina and J. Sayer, "Safety pilot model deployment: Test conductor team report," *Report No. DOT HS*, vol. 812, no. 171, p. 18, 2014.
- [56] Wikipedia contributors, "Hellinger distance," 2022. [Online]. Available: [https://en.wikipedia.org/wiki/Hellinger\\_distance](https://en.wikipedia.org/wiki/Hellinger_distance)
- [57] G. Grimmett and D. Stirzaker, *Probability and random processes*. Oxford university press, 2020.
- [58] Gurobi Optimization, LLC, "Gurobi Optimizer Reference Manual," 2022. [Online]. Available: <https://www.gurobi.com>
- [59] P. A. Lopez, M. Behrisch, L. Bieker-Walz, J. Erdmann, Y.-P. Flötteröd, R. Hilbrich, L. Lücken, J. Rummel, P. Wagner, and E. Wießner, "Microscopic traffic simulation using SUMO," in *2018 21st International Conference on Intelligent Transportation Systems (ITSC)*. IEEE, 2018, pp. 2575–2582.
- [60] VISSIM, "Vissim 5.40-01, User Manual," 2012, planung Transport Verkehr AG, Karlsruhe, Germany.
- [61] J. Erdmann, "Sumo lane-changing model," in *Modeling Mobility with Open Data*. Springer, 2015, pp. 105–123.
- [62] B. Hammit, R. James, and M. Ahmed, "A case for online traffic simulation: Systematic procedure to calibrate car-following models using vehicle data," in *2018 21st International Conference on Intelligent Transportation Systems (ITSC)*. IEEE, 2018, pp. 3785–3790.
- [63] B. Hammit, "A case for online traffic simulation: Systematic procedure to calibrate car-following models using vehicle data," <https://github.com/bhammit1/Analysis>, 2018.
- [64] S. E. Lee, E. C. Olsen, W. W. Wierwille *et al.*, "A comprehensive examination of naturalistic lane-changes," United States. Department of Transportation. National Highway Traffic Safety Administration, Tech. Rep., 2004.
- [65] National Highway Traffic Safety Administration, "FARS/CRSS coding and validation manual," *Report No. DOT HS*, vol. 813, no. 251, 2022.
- [66] E. de Gelder, J. Manders, C. Grappiolo, J.-P. Paardekooper, O. O. den Camp, and B. D. Schutter, "Real-world scenario mining for the assessment of automated vehicles," 2020.
- [67] W. J. Dixon and F. J. Massey Jr, *Introduction to statistical analysis*. McGraw-Hill, 1951.
- [68] E. Leurent, "An environment for autonomous driving decision-making," <https://github.com/eleurent/highway-env>, 2018.
- [69] X. Gong, Y. Guo, Y. Feng, J. Sun, and D. Zhao, "Evaluation of the energy efficiency in a mixed traffic with automated vehicles and human controlled vehicles," in *2018 21st International Conference on Intelligent Transportation Systems (ITSC)*. IEEE, 2018, pp. 1981–1986.
- [70] Federal Highway Administration (FHWA), *Highway Capacity Manual, Special Report 209*. Transportation Research Board, National Research Council, 1994.